

Performance Evaluation of Novel Concentrating Photovoltaic Thermal Solar Collector under Quasi-Dynamic Conditions

Sahand Hosouli ¹, João Gomes ^{1,2,*}, Muhammad Talha Jahangir ¹ and George Pius ³

¹ MG Sustainable Engineering AB, 75340 Uppsala, Sweden; sahand@mgsust.com (S.H.)

² Faculty of Engineering and Sustainable Development, University of Gävle, 80176 Gävle, Sweden

³ Absolicon Solar Collector AB, 87133 Härnösand, Sweden

* Correspondence: joao.santos.gomes@hig.se

Abstract: Concentrating Photovoltaic Thermal (CPVT) collectors are suitable for integration in limited roof space due to their higher solar conversion efficiency. Solar sunlight can be used more effectively by CPVT collectors in comparison to individual solar thermal collectors or PV modules. In this study, the experimental investigation of a novel CPVT collector called a PC (power collector) has been carried out in real outdoor conditions, and the test set-up has been designed based on ISO 9806:2013. A quasi-dynamic testing method has been used because of the advantages that this method can offer for collectors with a unique construction, such as the proposed collector, over the steady-state testing method. With a quasi-dynamic testing method, it is possible to characterize the collector within a wide range of incidence angles and a complex incidence angle modifier profile. The proposed novel collector has a gross area of 2.57 m². A maximum power output per collector unit area of 1140 W is found at 0 °C reduced temperature (1000 W/m² irradiance level), while at a higher reduced temperature (70 °C), it drops down to 510 W for the same irradiance level. The data have been fitted through a multiple linear regression method, and the obtained efficiency curve coefficients are 0.39, 0.192, 1.294, 0.023, 0.2, 0, −5929 and 0 for $K_{\theta d}$, b_0 , c_1 , c_2 , c_3 , c_4 , c_5 and c_6 , respectively. The experimental characterization carried out on the collector proved that the output powers calculated by using the obtained parameters of the quasi-dynamic testing method are in good agreement with experimental points.

Keywords: quasi-dynamic collector testing; photovoltaic-thermal; concentrating photovoltaic thermal; quasi-dynamic model; ISO 9806:2013



Citation: Hosouli, S.; Gomes, J.; Talha Jahangir, M.; Pius, G. Performance Evaluation of Novel Concentrating Photovoltaic Thermal Solar Collector under Quasi-Dynamic Conditions. *Solar* **2023**, *3*, 195–212. <https://doi.org/10.3390/solar3020013>

Academic Editor: Sungwoo Yang

Received: 9 January 2023

Revised: 15 March 2023

Accepted: 3 April 2023

Published: 11 April 2023



Copyright: © 2023 by the authors. Licensee MDPI, Basel, Switzerland. This article is an open access article distributed under the terms and conditions of the Creative Commons Attribution (CC BY) license (<https://creativecommons.org/licenses/by/4.0/>).

1. Introduction

Over the past four decades, global energy consumption has been steadily increasing, and today, the environment and energy are the two main issues for humanity. Fast population and industrial growth over the last two centuries have caused in a huge rise in energy demand, with an annual increasing rate of 2.3% from the year 1949 to 2009 [1]. In 2008, the total annual consumption of energy reached 474×10^{18} J, of which a very large majority (about 80–90%) comes from combustion of fossil fuels [2]. Emissions from consumption of fossil fuels are the primary reason for the rapid and accelerating growth in atmospheric CO₂, which is directly linked to global warming [1–3].

Among the available renewable energy sources, solar is one of the most promising sources of energy, as it supplies clean, environmentally friendly and abundant energy [4,5]. In 2012, solar photovoltaic (PV) energy provided for only 0.04% of total primary energy demand, while solar thermal energy provided 0.5% of energy supply. Future developments are expected to continue in solar photovoltaic and solar thermal technologies due to increased concerns around environmental protection, energy saving and CO₂ emissions [2,6].

The conversion efficiencies of PV systems such as silicon solar cells, III–V multi-junction solar cells and 4-junction solar cells (developed by the ISE Fraunhofer institute)

are 14–22, 25–30 and 46%, respectively [7,8]. Today, one issue to tackle in order to improve the operating conversion efficiencies of PV systems is avoiding performance losses due to the cell temperature coefficient, which is caused by solar cells heating up, since only a fraction of the light is converted into electricity.

In order to achieve higher area efficiency, the photovoltaic-thermal (PVT) technology and concept were developed and documented in the mid-1970s; this was followed by some experimental and theoretical studies [9–11].

A PVT collector is a single unit formed by a combination of photovoltaic (PV) and solar thermal technologies to generate electricity and heat from the same area [2,12,13]. PVT technology can result in higher solar conversion efficiency of the module, leading to better use of the limited roof space. In addition, solar sunlight can be used more effectively by PVT technology in comparison to the individual PV or solar collector technologies, and can lead to a higher overall solar conversion rate [2]. In recent decades, several experimental and theoretical investigations have focused on the utilization of PVT solar systems to develop technologies with high performance [14]. PVT collectors find practical use in both industrial and residential settings, with numerous applications such as water desalination, solar drying, water heating, space heating, solar cooling, and building integrated skins and facades, among others [6,15,16].

PVT systems can be classified in several different ways, such as their type of solar input (non-concentrated and concentrated), their applications, their working medium (water, air, water/air, nanofluids, thermic fluids and phase change materials), and the arrangement of heat extraction (natural circulation and forced circulation), etc. In non-concentrated PVT systems, solar radiations are used without any concentrating arrangements [6,9]. The performances of different water-based non-concentrated PVT systems have been analysed theoretically and experimentally in various research papers. Some examples of these systems are as follows: different arrangement of water channels [17–19]; collector surface-covering arrangement [20–24]; PVT systems with and without glazing [25]; semi-transparent PV modules [26,27]; use of phase change material [28]; systems with a multi-fluid and collector surface-covering arrangement [24,29].

Solar collectors such as linear Fresnel reflectors (LFR), parabolic trough collectors (PTC), and other concentrating collectors have great potential to improve the solar radiation gathering process for power generation [30] and industrial process heating with small-size parabolic trough collectors [31]. Since the early 1980s, CPVT systems with different types of solar concentrators and various solar materials have been an attractive area of solar research [32]. CPVT collectors can achieve high thermal and optical efficiencies, as well as lower energy costs and payback periods according to their performance. For instance, 2.37 \$/W and 8.7 \$/W are reported to be the cost of electricity and the total electrical and thermal costs of a CPVT collector, respectively [33,34].

Several studies have been conducted in the field of PVT and CPV systems. J.I. Rosell et al. [35] studied different concentrations of arrangements for small-scale PVT systems at the University of Lleida in Spain. In order to concentrate more radiation onto the PV cells, linear Fresnel lenses with two-axis tracking were used. The measured thermal performance, without electrical production, varies from 60% to 65% for the inlet temperature between 10 and 50 °C. The thermal behaviour was simulated by an analytical model and validated by experimental results. In another study, J.S. Coventry et al. [36] from the Australian National University analyzed in detail the performance of a parabolic PVT collector with mono-crystalline silicon cells attached to the receiver, using water as a heat transfer fluid. The combined efficiency achieved was 69% (58% thermal efficiency and 11% electrical efficiency). At Lund Technical University, L.R. Bernardo et al. [37] studied the performance of CPVT with PTC. The mono-crystalline PV modules were attached to the absorber, and a silver-coated plastic film laminated to a steel sheet was used as the reflective surface of the parabolic reflector. The obtained electrical and optical efficiencies were 6.4% and 0.4%, respectively. Another relevant study performed by M. Li et al. [38] investigates the performance of the CPVT system, with a 10 m² concentrating trough collector and

three types of solar cell arrays (a super cell array, a gallium arsenide (GaAs) cell and a concentrating silicon cell). The thermal and average electrical efficiencies of the system with a super cell array were found to be 45.17 and 3.63%, respectively. For the systems with a GaAs cell and silicon cell array, the thermal efficiencies were 41.69%, and 34.53%, respectively.

Researchers from Tunisia, Germany, India and USA have studied CPVT systems. M. Chaabane et al. [14] studied the performance and commercial application of a PVT system including a 3.64 m long trough concentrating collector made of stainless steel, and a 1.825 m long rectangular absorber conduit made of black coated steel. Some 18 mono-crystalline PV modules of 20 W were attached to the absorber. The overall efficiency achieved was 26% (16% thermal efficiency and 10.2% electrical efficiency). The CFD model of the system was also carried out and validated with experiments. In addition to ray-tracing simulations, M. Proell et al. [39] conducted an experimental study on a CPVT system in order to examine the impact of eight different CPC reflectors' geometries on the PV efficiency in in situ conditions. An aluminium thermal absorber with a c-Si cell was used, and an average of 10–11% electrical efficiency of was obtained. S. Sharma et al. [40] studied a CPVT system for building integration based on linear asymmetric compound parabolic collectors with LGBC (laser-grooved buried contact) crystalline silicon solar cells using phase change material (paraffin wax). At 1000 Wm^{-2} , through use of PCM, the obtained electrical efficiency was improved by 7.7%. Furthermore, a novel optimized mathematical model for a building-integrated concentrating photovoltaic-PCM system was also presented. B.K. Widyolar et al. [41] designed, fabricated and tested a CPVT system equipped with PTC and a non-imaging compound parabolic concentrator (CPC) with a gallium arsenide (GaAs) solar cell. In the experimental setup, the obtained maximum outlet temperature, thermal efficiency and electric efficiency from the GaAs cells were $365 \text{ }^\circ\text{C}$, 37% and 8%, respectively. In addition to performance analysis of basin-type solar still-integrated systems with a PVT-CPC, D.B. Singh et al. [42,43] investigates the productivity and enviro-economic and exergo-economic parameters of single and double-slope PVT-CPC solar distillation systems. Coated aluminium sheets were used to make the CPC collectors. The receiver area is half of the aperture area, and the obtained annual productivity showed that the system feasible from an energy point of view.

To forecast the energy production of diverse solar thermal systems, it is crucial to have knowledge about the thermal efficiency of a broad range of solar collector technologies. Numerous standards exist that can assess the efficiency of solar thermal collectors, irrespective of their technology. Some examples are: EN 12975-2 [44], EN 12976 [45], EN 12977 [46], ASHRAE 93 [47], ASTM E905-87:2013 [48], SRCC 600 2014-07 [49] and ISO 9806:2017 [50]. However, it is important to note that the SRCC 600 2014-07 standard has a relatively high degree of similarity to ISO 9806 standard. Two different test approaches are proposed by the aforementioned standards for characterizing the thermal performance of solar thermal collectors: the quasi-dynamic test (QDT) and the steady-state test (SST) [51].

To conduct the SST method, it is crucial to keep all pertinent parameters for thermal performance constant within the permissible range of values defined by the standard during measurements. Additionally, the test must be carried out under clear sky conditions, with a low level of diffuse radiation. Consequently, the SST method model does not have a correction term for diffuse radiation, and normal incidence radiation is utilized to determine the efficiency curve parameters [44,51,52].

On the other hand, the QDT method necessitates less involvement from the operator. Additionally, fewer sunny days are necessary to perform the QDT method successfully, as compared to the SST method [52]. Moreover, the QDT method provides a more comprehensive depiction of the collector compared to the SST method, as it incorporates correction terms, such as wind speed and long-wavelength radiation incident on the collector in certain cases. To execute the QDT method, tests must be conducted for a minimum of 3 h under varying sky conditions [44,49–51]. Since the SST and QDT methods share similar principles, there is no clear basis for choosing one over the other [53]. In addition, several

standards are available for PV systems, including IEEE (1262 and 929) [54,55], UL (1703, 1741 and 4703) [56–58], IEC (61215, 61646, 61730) [59–62] and other national electric codes.

This paper aims to introduce the concept of a novel CPVT collector in addition to a detailed description of a collector test stand based on ISO 9806:2013 for evaluating its thermal performance using the QDT method. Previous studies on the thermal performance evaluation of novel CPVT designs were limited. Although CPVT technology has received increasing attention during the past decade, limited studies have been conducted on testing methods of novel CPVT collector designs. This study presents a detailed testing procedure of a novel CPVT collector called PC, based on QDT method. Testing according to the QDT method over the SST method is a result of the advantages that the QDT method offers, especially for collectors with a unique construction such as the proposed CPVT collector. Using the QDT method, it is possible to characterize the collector within a wide range of incidence angles and a complex incidence angle modifier (IAM) profile.

2. Materials and Methods: Components and Performance Analysis of Novel CPVT Collector (PC)

2.1. Description of Collector

Figure 1 shows an expanded view of the proposed novel CPVT collector. It is a concentrating hybrid solar photovoltaic and solar thermal panel (CPVT). The collector is concentrating due to its curved mirror that reflects and concentrates the sunlight on to the bottom side of the receiver of the collector. This reflector geometry is called MaReCo, and has been published elsewhere [63]. The collector combines solar photovoltaic (PV) generation of electricity with solar thermal (T) generation heat and therefore is a hybrid concept. The manufacturer states that the collector has a thermal efficiency of 52%, and a linear loss coefficient of $3.47 \text{ W}/(\text{m}^2 \cdot \text{K})$ [64].

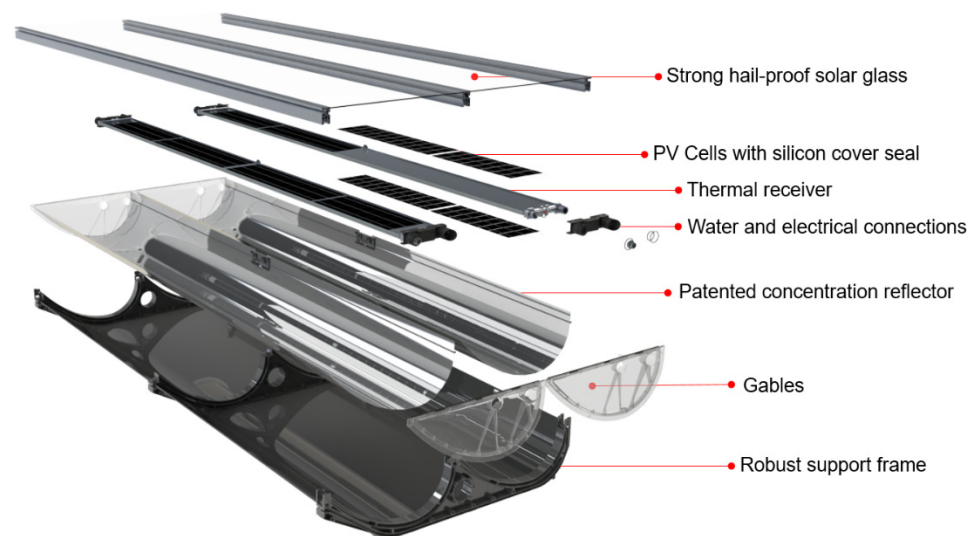


Figure 1. Proposed novel CPVT collector (PC).

The total size of the PC is $2.31 \times 0.955 \text{ m}$, and it consists of two major components: the collector box and the receiver core. The box contains the concentrating mirrors and houses the receiver. The collector box can be sub-divided into four components, as follows:

A black plastic frame, which is made of support ribs and a covering sheet of plastic.

The transparent gables, which are constructed from polymethyl-methacrylate (PPMA) and provide sealing for both sides of the collector. The manufacturer guarantees a transparency of 90%.

Tempered solar glass, which has a thickness of 4 mm and is treated with an anti-reflective coating on both sides to reach an absorptance of 1.5% and a reflectance of 2% per side.

An aluminium reflector, which consists of a compound parabolic and circular reflective sections that concentrate the solar radiation onto the receiver. It has a reflectance of 92% and achieves a concentration ratio of 1.7 with this particular geometry. Studies from M. Rönnelid et al. and M. Adsten et al. [63,65] describe the geometry of the reflector in more detail.

With a length of 2321 mm, a width of 165 mm, and a thickness of 14.5 mm, the aluminium receiver contains solar cells on both of its sides, as depicted in Figure 2. These solar cells are encapsulated in highly transparent silicone with a reported transparency of 97%.



Figure 2. Receiver core design of novel CPVT collector (PC).

As shown in Figure 3, the receiver comprises an aluminium structure containing eight elliptical channels, through which the cooling fluid flows to extract heat from the collector. The core of the receiver is made from extruded aluminium.

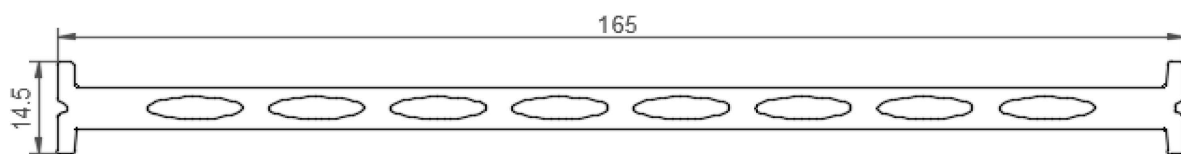


Figure 3. Elliptical channels in receiver.

Utilizing standard monocrystalline solar silicon cells with an efficiency of 19.7%, the collector has a cell string layout of four strings at the bottom and four at the top side of the receiver, as shown in Figure 4.



Figure 4. Receiver, showing four cell strings and its distribution in the receiver.

2.2. Description of Collector Test Rig

To conduct tests using the QDT method, a solar thermal collector test rig was established on a rooftop, in compliance with the European standard EN 12975-2:2006 (the predecessor to the present ISO standard). Figure 5 depicts a rotatable mounting platform that was used for the installation and testing of thermal collectors on the rooftop. The test rig is located at latitude and longitude of 60.48° and 15.44° , respectively. The collector azimuth is 0° .



Figure 5. Rooftop collector mounting stand.

The test rig includes an advanced hydraulic circuit that can maintain testing conditions for two distinct collectors and is designed in accordance with the circuit layout recommended by the ISO 9806:2013 standard. All test measurements are captured by a data acquisition device, which is linked to a computer that records the readings every 10 s. A diagram of the data measurement and logging system is shown in Figure 6, while Table 1 provides information on the temperature and flow regulation system.

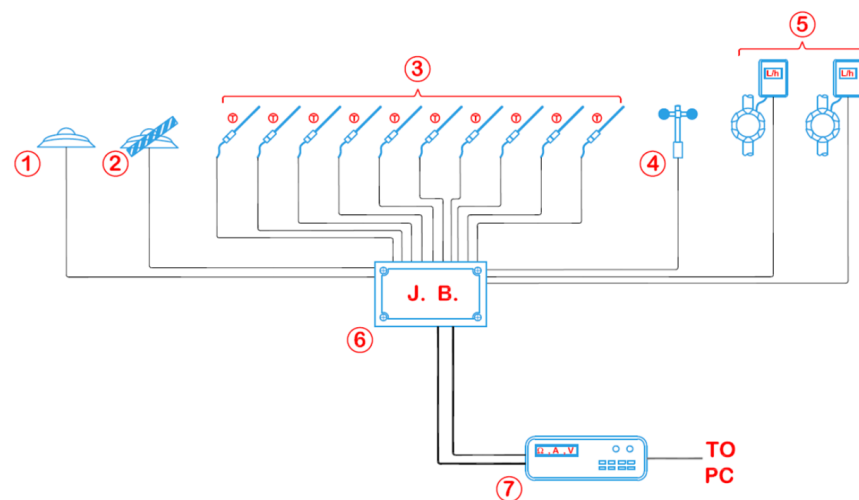
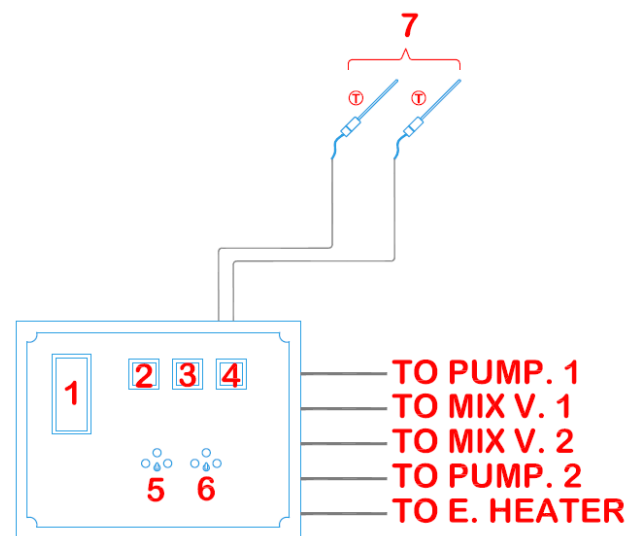


Figure 6. Data measurement and logging system.

To maintain the operational set values, a temperature and flow regulation control panel is utilized, which is depicted in Figure 7. The control panel allows for the regulation of the pump speed, heating and cooling elements, to achieve the required test boundaries set by the standard. Additionally, Table 2 provides specifics about the temperature and flow regulation system.

Table 1. Details of temperature and flow regulation system.

Item No.	Description	Manufacturer	Model	Relevant Info
1	Pyranometer	Kipp & Zonen	CM11	Industry standard for monitoring and logging solar irradiance Sensitivity $7 \mu\text{V}\cdot\text{W}^{-1}\cdot\text{m}^{-2} - 14 \mu\text{V}\cdot\text{W}^{-1}\cdot\text{m}^{-2}$ Non-linearity $< 0.2\%$
2	Pyranometer with shading ring	Kipp & Zonen	CM11	4 wire RTD sensor, individually calibrated
3	Temperature sensors	Unknown	PT100	Accuracy $\pm 0.5 \text{ m}\cdot\text{s}^{-1}$ Resolution $< 0.1 \text{ m}\cdot\text{s}^{-1}$ Range $0.5 \text{ m}\cdot\text{s}^{-1} - 50 \text{ m}\cdot\text{s}^{-1}$
4	Wind speed sensor	Thies Clima	N/A	Electromagnetic flow sensor Accuracy $\pm 0.3\%$ of mean value
5	Flow sensors	Krohne	IFC 300	Electrically actuated mixing valve controlled by the borehole cooling control unit to regulate the coolant fluid flow from the borehole
6	Junction box			
7	Data logging device	Agilent Technologies	34972A	Highly sophisticated programmable data measurement, and export device capable of high-resolution voltage, current, and resistance measurements simultaneously with PC interface for logging

**Figure 7.** Temperature and flow regulation system.

2.3. QDT Testing Procedure

Though testing under SST conditions can yield useful results, testing under dynamic conditions using the QDT method offers characterization of a different type of collectors under a wider range of operating and ambient conditions. In addition, more complete and complex characterization of collectors is achievable with the QDT method. Looking at the thermal collector model under the QDT procedure, the quasi-dynamic thermal collector model equation, as adapted by the ISO 9806:2013, can be identified by Equation (1).

$$\begin{aligned} \frac{\dot{Q}}{A} = & \eta_{0,b}K_{\theta b}(\theta_L, \theta_T)G_b + \eta_{0,b}K_{\theta d}G_d - c_1(T_m - T_a) - c_2(T_m - T_a)^2 \\ & - c_3u(T_m - T_a) + c_4(E_L - \sigma T_a^4) - c_5\frac{dT_m}{dt} - c_6uG \end{aligned} \quad (1)$$

Table 2. Details of temperature and flow regulation system.

Item No.	Description	Manufacturer	Model	Relevant Info
1	Pump control panel	Danfoss	2216e	Frequency drive pump controller regulating the primary pump (Pump. 1) flow rate
2	Heater control unit	Eurotherm	2216e	PID controller regulating operation of the system's electrical heating elements based on a temperature set point, temperature signal is taken from an RTD sensor located in line after the heating element
3	Control unit-cooling circuit 1	Eurotherm	2216e	PID controller regulating operation of the system's borehole cooling pump (Pump. 2) and mixing valve (Mix V. 1) based on a temperature set point; temperature signal is taken from an RTD sensor located in line after the cooling circuit heat exchanger.
4	Control unit-cooling circuit 2	Eurotherm	2216e	Unused heat pump cooling circuit controller
5	Mixing valve-cooling circuit 1			Electrically actuated mixing valve controlled by the borehole cooling control unit to regulate the coolant fluid flow from the borehole
6	Mixing valve-cooling circuit 2			Unused heat pump cooling circuit mixer
7	Temperature sensors	Unknown	PT100	2 RTD sensor, one after the heating element, and one after cooling circuit 1

The model includes various coefficients: c_1 represents the heat loss coefficient when the temperature difference between T_m and T_a is zero, c_2 accounts for the temperature dependence of the heat loss coefficient, c_3 considers the wind speed dependence of the heat loss coefficient, c_4 represents the dependence of the heat loss coefficient on the long wave irradiance, c_5 is the effective thermal capacitance, and c_6 accounts for the wind speed dependence of the zero loss efficiency. $K_b(\theta_L, \theta_T)$ is the IAM for beam radiation, and defined as $K_b(\theta_L, \theta_T) = 1 - b_0((1/\cos\theta) - 1)$ [50,66]. To test the performance of the PC using the QDT method, full-day tests covering all possible day sequences were carried out for a total of 17 days, and data were recorded every 10 s. The collected raw data, which comprised roughly 145,000 data points, were filtered to remove any unusable data. The input values were averaged over a 10 min period to determine the thermal capacitance. The data were then visually inspected to ensure that they met the QDT criteria. Only 262 conditioned and averaged points were used to characterize the collector by MLR (multiple linear regression) to determine the required coefficients. Figure 8 shows that the chosen data entry points cover five different inlet temperature levels and the data points are spread over a slightly narrow range of irradiance levels, with not many points over 800 W/m^2 . As a first step of visual inspection, it is ensured that all the inlet temperatures tested can be identified. In addition, wind speed, deviation of measured inlet temperature, the average value of measured mass flux and the irradiation distribution over the incidence angles were checked.

Table 3 presents the proposed test conditions and the permitted deviations from average values by ISO 9806:2013, based on the QDT method. In addition, the proposed limits based on the SST method also presented for comparison.

Figure 9 shows the wind speed distribution over the range of irradiance that is needed to confirm the diversity of the wind speed data; it is in the range of 0–4 m/s, as imposed by the standard in the QDT method.

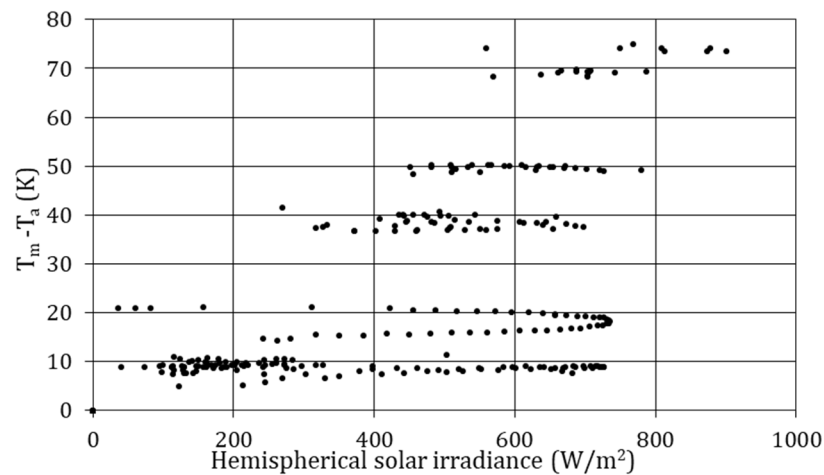


Figure 8. Reduced temperature ($T_m - T_a$) versus the total irradiance.

Table 3. Test conditions and permitted deviations from average values based on QDT and SST methods.

Variable	QDT Method		SST Method	
	Value	Deviation	Value	Deviation
Global radiation G [W/m^2]	-	-	>700	± 50
Incidence angle θ [$^\circ$]	-	-	<20	-
Diffuse fraction G_d/G [%]	-	-	<30	-
Ambient temperature T_a [K]	-	-	-	± 1.5
Wind speed u [m/s]	$1 < u < 4$	-	$2 < u < 4$	-
Inlet temperature T_{in} [K]	-	± 1	-	± 0.1
Mass flux \dot{m} [$kg \cdot s^{-1} \cdot m^{-2}$]	0.02	$\pm 1\%$	0.02	$\pm 1\%$

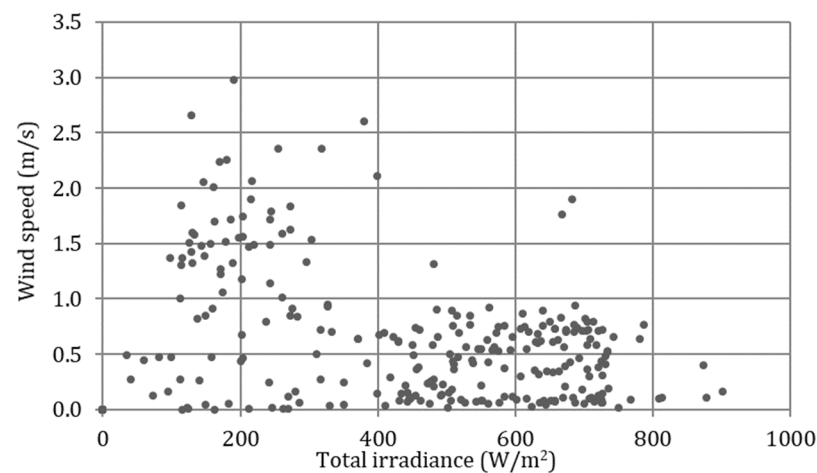


Figure 9. Wind speed distribution over the range of irradiance.

During the thermal efficiency measurements of PC, the deviation of the inlet temperature of collector is less than 1 K for all test points. Furthermore, the mass flux is fixed at $0.02 \text{ kg} \cdot \text{s}^{-1} \cdot \text{m}^{-2}$, with deviation under 1% (as proposed by ISO 9806:2013 based on QDT method).

In addition, based on ISO 9806:2017, the standard specific heat capacity of water at 1 to 12 bars is a polynomial function of the average temperature of the heat transfer fluid. Therefore, the uncertainty of the C_p is smaller than 0.04%.

In order to obtain a complex collector model that has the incident angle modifiers for the full range to be validated over any given incident angel, the distribution of direct

and diffuse irradiation over the full range of incidence angles is necessary. Furthermore, this will have a more pronounced effect in modelling of collectors. Figure 10 shows the distribution of direct and diffuse irradiation over the full range of incidence angles for PC.

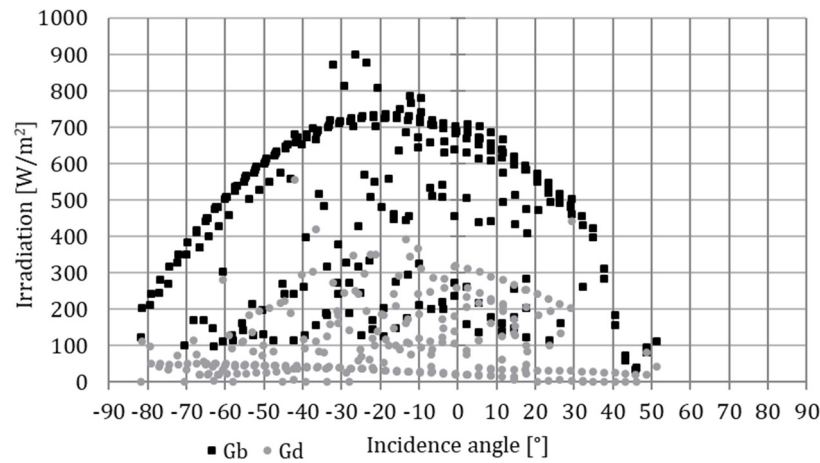


Figure 10. Irradiation distribution over the incidence angles.

3. Results & Discussion

3.1. QDT Testing Results

The MLR method is the most widely used mathematical tool and referred to in the EN 12975-2 standard. In this method, the equation is written as a sum of functions weighted by the parameters to be determined and can be highly nonlinear [66,67].

For unglazed collectors, all the model parameters presented in Equation (1) are required. For glazed collectors, the wind-induced losses and the long wave radiation both have negligible weight in the absolute losses and gains; therefore, they are often recommended to be omitted at the start (c_3, c_4 and c_6). However, since the wind speed has been measured and recorded, this study considers it.

The gross area of PC is 2.57 m², and the fluid flow rate used for the tests is fixed at 0.04 kg/s. Figure 11 shows the power output of PC per collector unit for three different irradiance levels. The obtained peak power per collector unit is 1140 W.

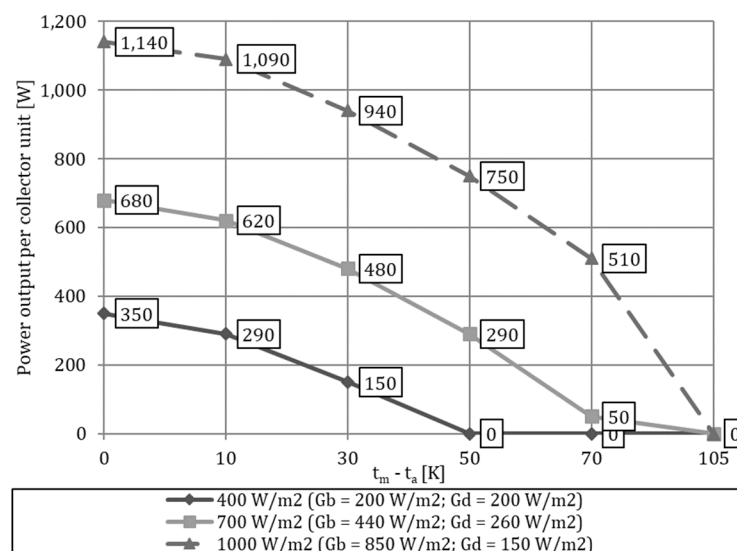


Figure 11. Power output per collector unit area.

MLR adjusts a set of N experimental points (\bar{x}_i, y_i) as a linear combination of M arbitrary functions $X_k(\bar{x})$, and the objective of the adjustment is to minimize the merit function (χ^2) (Equations (2) and (3)).

$$y(\bar{x}) = \sum_{k=1}^M a_k X_k(\bar{x}) \quad (2)$$

$$\chi^2 = \sum_{i=1}^N \left[\frac{y_i - \sum_{k=1}^M a_k X_k(\bar{x}_i)}{u_i} \right]^2 \quad (3)$$

The least-squares method assumes that the uncertainty of the experimental point (u_i) remains constant, whereas in reality, each data point has its own uncertainty which almost never remains constant for all observations. Therefore, the weighted least-squares method is more appropriate for fitting the measurement data [68–70]. The contributions to the uncertainty of the thermal efficiency are calculated, and the use of calibrated RTD Pt100s ensures that the uncertainties of inlet and outlet temperature evaluations for the given set-up are low, even at high temperatures, with a contribution of 21.5% to the uncertainty of ΔT . The measurement of radiation accounts for about three-quarters of the uncertainty contribution, while the contribution to the uncertainty of other measured values on thermal efficiency is less than 3%. Since the uncertainty values were very small compared to their measured quantities (due to proper measurement device selection and system design), the combined standard absolute uncertainty for the thermal efficiency obtained by propagating the errors is less than 0.8%. In Equation (3), u_i^2 is the variance of the difference, and this weighting uncertainty is calculated by Equation (4) for uncertainty in x (the independent variable) and in y (the dependent variable).

$$u_i^2 = u_y^2 + \sum \left(\frac{\partial y}{\partial x_i} \right)^2 \cdot u_{x_i}^2 \quad (4)$$

Therefore, Equation (3) is nonlinear, and the Levenberg–Marquardt method can be used to identification of parameters. However, the least-squares method is also acceptable to use in order to first obtain a new set of parameters from which one calculates the uncertainties [44,45]. Table 4 shows the regression parameters related to Equation (1), and their standard deviation-based MLR method. In addition, the change in the thermal performance of the collector resulting from the incident angle is called the incident angle modifier (IAM) $K_\theta(\theta)$. With the QDT method, $K_\theta(\theta)$ is defined as two distinct parameters for diffuse and direct radiation. The term for direct radiation, $K_{\theta b}(\theta)$, is modelled as a function of the incident angle, and the term for diffuse radiation, $K_{\theta d}$, is modelled as a constant value. Table 5 shows the incident angle modifier values for direct radiation ($K_{\theta b}(\theta)$) as a function of the incident angle.

Table 4. Details of temperature and flow regulation system.

Coefficient	Value	Standard Deviation	Unit
$\eta_{0,b}$	48.9	3%	%
$K_{\theta d}$	0.38	9%	%
b_0	0.192	3%	
c_1	1.294	−20%	W/(K·m ²)
c_2	0.023	−14%	W/(K ² ·m ²)
c_3	0.2	−74%	W·s/(m ³ ·K)
c_4	0		
c_5	5929	38%	J/(K·m ²)
c_6	0		

Table 5. Incident angle modifier values for direct radiation ($K_{\theta b}(\theta)$).

θ	10	20	30	40	50	60	70	80
$K_{\theta b}$	0.96	0.94	0.96	0.95	0.89	0.78	0.71	0.46

Figure 12 shows that the actual measured power production and production calculated using the extracted parameters are in harmony, and this indicates a successful parameterization.

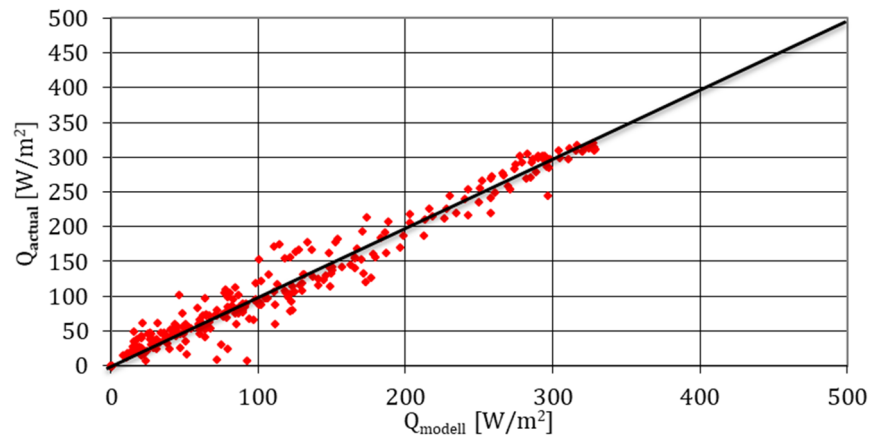


Figure 12. Actual measured production compared to model predicted generation.

Figure 13 shows the power output of the PC per collector unit using the obtained parameters of QDT (mentioned in Table 5) at 1000 W/m² hemispherical irradiance with no diffuse radiation. The wind speed is 3 m/s, and there is zero incidence angle for the zero loss efficiency. The results from the previous study based on the SST method and performed at AEL are also presented in Figure 13. The efficiency curve coefficients, including η , a_1 and a_2 , obtained from SST method in AEL, are 0.496, 3.155 W/m²·K and 0.022 W/m²·K², respectively. Further details on the AEL test mentioned in this part can be found in [71].

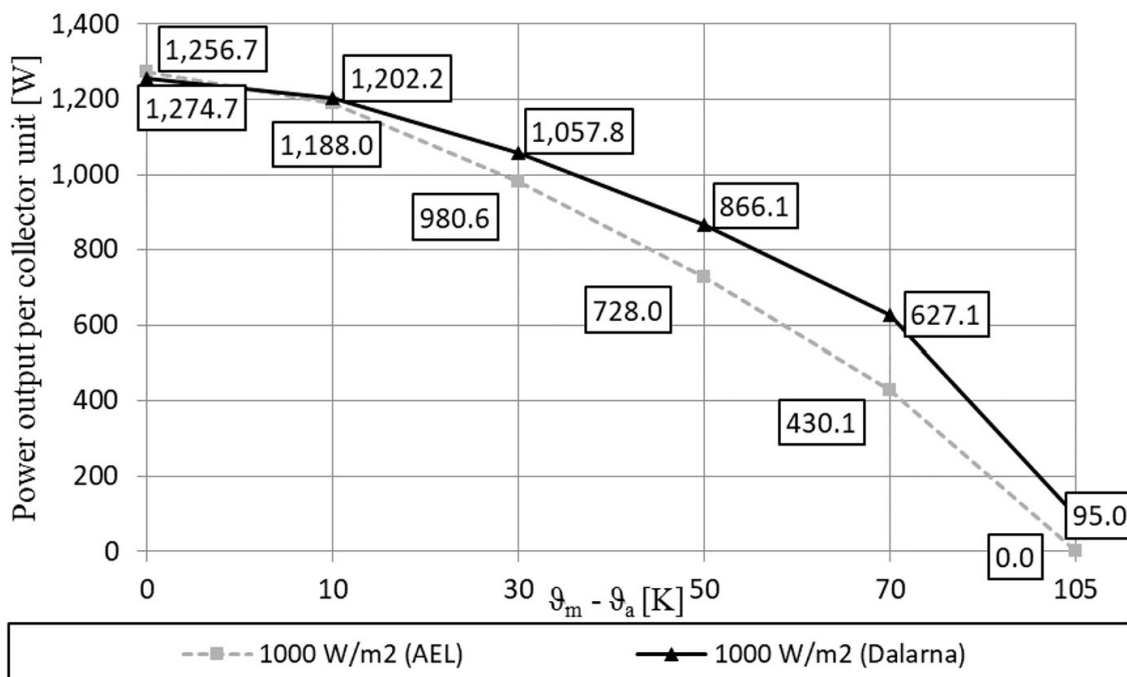


Figure 13. Power output per collector unit plotted from obtained parameters of QDT.

3.2. Thermal Efficiency Comparison

Figure 14 shows the thermal efficiency of the proposed novel CPVT collector in comparison with commercially available PVT technologies at a total solar irradiance of 800 W/m^2 , as a function of the difference between the mean solar collector fluid temperature of the PVT panel and the ambient air temperature. The proposed CPVT collector in this study proved to be the most promising solution at elevated temperatures, in comparison with commercially available non-concentrating PVT technologies [13].

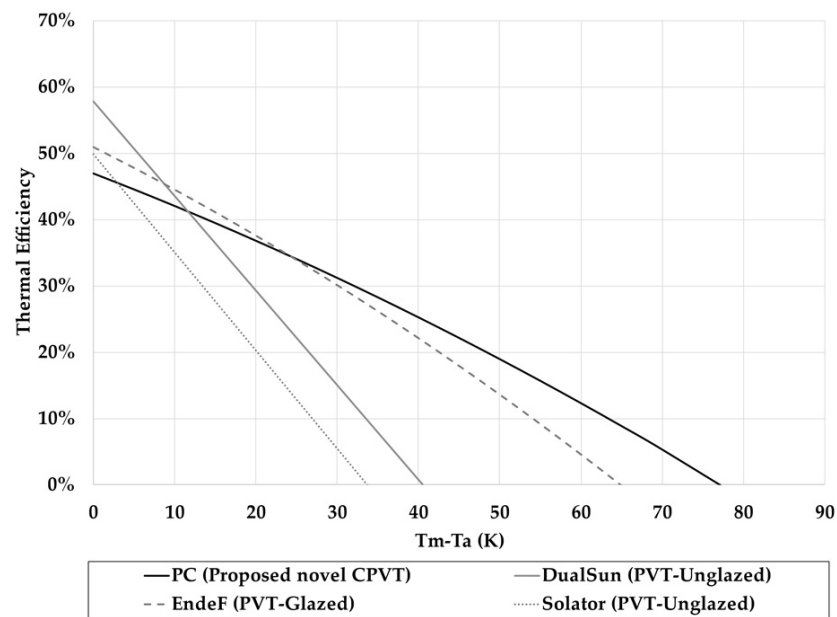


Figure 14. Thermal efficiency comparison between PC and commercially available PVT panels.

3.3. Thermodynamic Performance Evaluation

To evaluate the thermodynamic performance of novel CPVT collector (PC), a 3-D CAD model of receiver was created in Solidworks, and then imported into the ANSYS Structural Workbench for steady-state analysis. The thermodynamic performance was carried out by calculating the temperature distribution within a solid structure caused by thermal inputs (heat loads), outputs (heat loss), and thermal barriers (thermal contact resistance) in the design, using the finite element method. The thermal structural analysis addresses the conjugate heat transfer problem by simulating thermal conduction, convection, and radiation. In this study, structural analysis is carried out using the ANSYS Structural Workbench. The boundary conditions applied are a global solar irradiance of 750 W/m^2 , a convection heat transfer (with ambient air) of $5 \text{ W/m}^2\cdot\text{K}$, and a perfectly insulated bottom part of the collector. For this analysis, additional boundary conditions and constraints are required to specify how the collector is held within its frame and overall structure. The collector is assumed to be fixed with its frame at the collector water inlet. The temperature distribution is uniform in the layers, and the optical and thermal properties of the materials and fluids are constant. In this model, no surrounding shading is taken into account, the ambient temperature is constant around the receiver, and solar irradiance and wind speed are uniform over the collector's surface area. In addition, the total water mass flow rate is distributed uniformly amongst all collector channels with a uniform inlet temperature. Figure 15 shows the equivalent 1-D thermal resistance circuit and heat flow for the PC receiver.

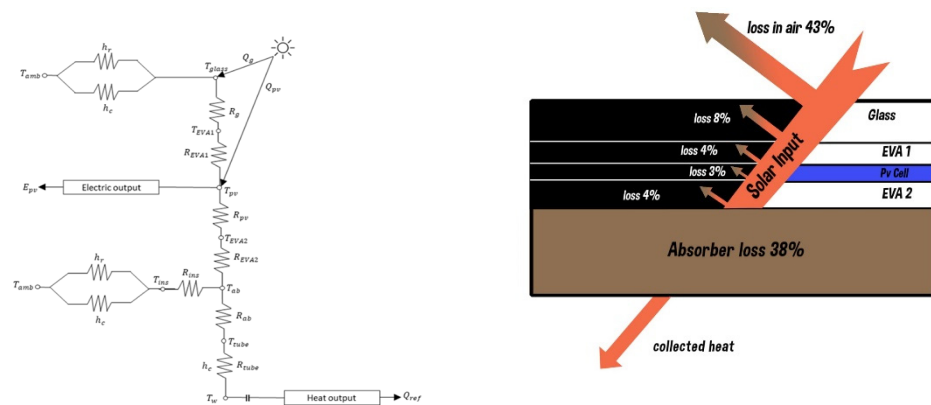


Figure 15. Equivalent 1-D thermal resistance circuit and heat flow for the PC receiver.

3.4. Cost Assessment of Novel CPVT Collector

A simple cost assessment was carried out on the application of the proposed novel CPVT collector (PC) in a dairy farm at LVAT-ATB in Germany, within a project called RES4LIVE under European Union’s Horizon 2020 research and innovation program [72]. The total estimated annual thermal energy demand at LVAT-ATB is 52,197 kW·h, and the proposed solar system integrates 24 PC collectors. Cost savings calculations over each year and the payback period of the system have been made, with the total system price known and the amount saved. The total investment for a system with 24 PC collectors is EUR 34,000. The annual thermal production of collectors running at a mean design temperature of 45 °C is 14,151 kW·h, and the annual electrical output is 4264 kW·h. Figure 16 shows the cash flow of investment in 24 PC collectors at the LVAT-ATB farm. The payback period is less than 6 years, and due to the higher heat production of the proposed PC collector at elevated temperatures, the payback period is lower than common commercial PVT collectors, even if there is a higher investment and maintenance cost [72].

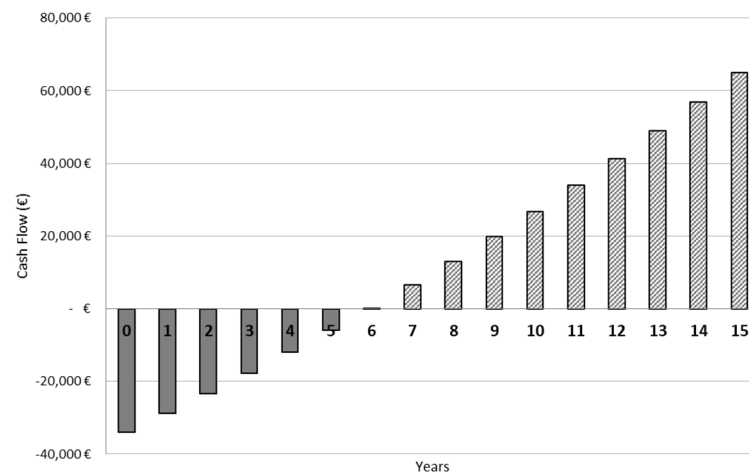


Figure 16. Cash flow of investment in 24 PC collectors for a system with a total estimated annual thermal energy demand of 52,197 kW·h.

4. Conclusions

In order to test the thermal performance of a collector in real outdoor conditions, the given test set-up, based on ISO 9806:2013, has been designed. The results of the tested PC in outdoor conditions show the behaviour of its performance at increasing temperatures, and the tests are based on experimental implementation of the QDT method. The PC has a gross area of 2.57 m², and a maximum power output of 1140 W per collector unit is found at a reduced temperature of 0 °C (1000 W/m² irradiance level), while at a higher reduced temperature (70 °C), it drops down to 510 W for the same irradiance level. The

data have been fitted through a multiple linear regression (MLR) method, and efficiency curve coefficients have been obtained. Based on the MLR Fit $K_{\theta d}$, b_0 , c_1 , c_2 , c_3 , c_4 , c_5 and c_6 are 0.39, 0.192, 1.294, 0.023, 0.2, 0, -5929 and 0, respectively. The experimental characterization carried out on the PC proved that the output powers calculated using the obtained parameters of the QDT method are in good agreement with experimental points.

Author Contributions: Conceptualization, S.H., J.G. and G.P.; methodology, S.H., J.G. and G.P.; writing—original draft preparation, S.H. and J.G.; writing—review and editing, S.H., M.T.J. and J.G. All authors have read and agreed to the published version of the manuscript.

Funding: This research was funded by RES4LIVE (Energy Smart Livestock Farming towards Zero Fossil Fuel Consumption—Grant Agreement No. 101000785), Res4Build (Renewables for clean energy buildings in a future power system—Grant Agreement No. 814865) and PowerUpMyHouse (Grant Agreement No. 2020-1-TR01-KA202-093467).

Informed Consent Statement: Informed consent was obtained from all subjects involved in the study.

Data Availability Statement: Data will be made available on request.

Conflicts of Interest: The authors declare no conflict of interest.

Abbreviations

PV	Solar photovoltaic
PVT	Photovoltaic-thermal
CPVT	Concentrating photovoltaic Thermal
PTC	Parabolic trough collector
CPC	Compound parabolic concentrator
SST	Steady-state test
QDT	Quasi-dynamic test
PPMA	Polymethyl methacrylate
TC	Thermocouples
RTD	Resistance temperature detector
MLR	Multiple linear regression
IAM	Incident angle modifier

Variables

G	Global radiation [W/m^2]
G_b	Direct solar irradiance (beam irradiance) [W/m^2]
G_d	Diffuse solar irradiance [W/m^2]
θ	Incidence angle [$^\circ$]
G_d/G	Diffuse fraction [%]
T_a	Ambient temperature [K]
T_{in}	Inlet temperature [K]
T_m	Mean temperature of heat transfer fluid [K]
A	Gross area of the collector [m^2]
\dot{m}	Mass flux [$\text{kg}/\text{s}\cdot\text{m}^2$]
u	Wind speed [m/s]
c_1	Heat loss coefficient at $(T_m - T_a) = 0$ [$\text{W}/\text{m}^2\cdot\text{K}$]
c_2	Temperature dependence of the heat loss coefficient [$\text{W}/\text{m}^2\cdot\text{K}^2$]
c_3	Wind speed dependence of the heat loss coefficient [$\text{J}/\text{m}^3\cdot\text{K}$]
c_4	Sky temperature dependence of the heat loss coefficient [-]
c_5	Effective thermal capacity [$\text{J}/\text{m}^2\cdot\text{K}$]
c_6	Wind dependence in the zero loss Efficiency [s/m]
$K_{\theta b}(\theta_L, \theta_T)$	Incidence angle modifier for direct radiation [-]
$K_{\theta d}$	Incidence angle modifier for diffuse radiation [-]
b_0	Constant for the calculation of the incident angle modifier
η	Collector efficiency, with reference to reduced temperature difference
$\eta_{0,b}$	Peak collector efficiency reference to reduced temperature difference, based on beam irradiance G_b

References

1. Zhou, D.; Zhao, C.-Y.; Tian, Y. Review on Thermal Energy Storage with Phase Change Materials (PCMs) in Building Applications. *Appl. Energy* **2012**, *92*, 593–605. [[CrossRef](#)]
2. Zhang, X.; Zhao, X.; Smith, S.; Xu, J.; Yu, X. Review of R&D Progress and Practical Application of the Solar Photovoltaic/Thermal (PV/T) Technologies. *Renew. Sustain. Energy Rev.* **2012**, *16*, 599–617.
3. Canadell, J.G.; Le Quéré, C.; Raupach, M.R.; Field, C.B.; Buitenhuis, E.T.; Ciais, P.; Conway, T.J.; Gillett, N.P.; Houghton, R.A.; Marland, G. Contributions to Accelerating Atmospheric CO₂ Growth from Economic Activity, Carbon Intensity, and Efficiency of Natural Sinks. *Proc. Natl. Acad. Sci. USA* **2007**, *104*, 18866–18870. [[CrossRef](#)]
4. Loni, R.; Kasaeian, A.B.; Asli-Ardeh, E.A.; Ghobadian, B.; Le Roux, W.G. Performance Study of a Solar-Assisted Organic Rankine Cycle Using a Dish-Mounted Rectangular-Cavity Tubular Solar Receiver. *Appl. Therm. Eng.* **2016**, *108*, 1298–1309. [[CrossRef](#)]
5. Cuce, E.; Cuce, P.M.; Bali, T. An Experimental Analysis of Illumination Intensity and Temperature Dependency of Photovoltaic Cell Parameters. *Appl. Energy* **2013**, *111*, 374–382. [[CrossRef](#)]
6. Sultan, S.M.; Efzan, M.N.E. Review on Recent Photovoltaic/Thermal (PV/T) Technology Advances and Applications. *Sol. Energy* **2018**, *173*, 939–954. [[CrossRef](#)]
7. Wenham, S.R. *Applied Photovoltaics*; Routledge: Oxford, UK, 2011; ISBN 1849711410.
8. Philipps, S.P.; Bett, A.W.; Horowitz, K.; Kurtz, S. *Current Status of Concentrator Photovoltaic (CPV) Technology*; National Renewable Energy Lab. (NREL): Golden, CO, USA, 2015.
9. Joshi, S.S.; Dhoble, A.S. Photovoltaic-Thermal Systems (PVT): Technology Review and Future Trends. *Renew. Sustain. Energy Rev.* **2018**, *92*, 848–882. [[CrossRef](#)]
10. Chow, T.T. A Review on Photovoltaic/Thermal Hybrid Solar Technology. *Appl. Energy* **2010**, *87*, 365–379. [[CrossRef](#)]
11. Wolf, M. Performance Analyses of Combined Heating and Photovoltaic Power Systems for Residences. *Energy Convers.* **1976**, *16*, 79–90. [[CrossRef](#)]
12. Hosouli, S.; Cabral, D.; Gomes, J.; Kosmadakis, G.; Mathioulakis, E.; Mohammadi, H.; Loris, A.; Naidoo, A. Performance Assessment of Concentrated Photovoltaic Thermal (CPVT) Solar Collector at Different Locations. In Proceedings of the ISES SWC 2021 Solar World Congress Virtual Conference, Online, 25–29 October 2021; ISES: Freiburg im Breisgau, Germany, 2021.
13. Furbo, S.; Perers, B.; Dragsted, J.; Gomes, J.; Gomes, M.; Coelho, P.; Yıldızhan, H.; Halil Yilmaz, İ.; Aksay, B.; Bozkurt, A. Best Practices for PVT Technology. In Proceedings of the ISES SWC 2021 Solar World Congress Virtual Conference, Online, 25–29 October 2021; ISES: Freiburg im Breisgau, Germany, 2021.
14. Chaabane, M.; Charfi, W.; Mhiri, H.; Bournot, P. Performance Evaluation of Concentrating Solar Photovoltaic and Photovoltaic/Thermal Systems. *Sol. Energy* **2013**, *98*, 315–321. [[CrossRef](#)]
15. Charron, R.; Athienitis, A.K. Optimization of the Performance of Double-Facades with Integrated Photovoltaic Panels and Motorized Blinds. *Sol. Energy* **2006**, *80*, 482–491. [[CrossRef](#)]
16. Tripanagnostopoulos, Y. Aspects and Improvements of Hybrid Photovoltaic/Thermal Solar Energy Systems. *Sol. Energy* **2007**, *81*, 1117–1131. [[CrossRef](#)]
17. Huang, W.; Hu, P.; Chen, Z. Performance Simulation of a Parabolic Trough Solar Collector. *Sol. Energy* **2012**, *86*, 746–755. [[CrossRef](#)]
18. Zondag, H.A.; De Vries, D.W.; Van Helden, W.G.J.; Van Zolingen, R.J.C.; Van Steenhoven, A.A. The Yield of Different Combined PV-Thermal Collector Designs. *Sol. Energy* **2003**, *74*, 253–269. [[CrossRef](#)]
19. Ben Cheikh El Hocine, H.; Touafek, K.; Kerrou, F. Theoretical and Experimental Studies of a New Configuration of Photovoltaic-Thermal Collector. *J. Sol. Energy Eng.* **2017**, *139*, 021012. [[CrossRef](#)]
20. Mishra, R.K.; Tiwari, G.N. Energy and Exergy Analysis of Hybrid Photovoltaic Thermal Water Collector for Constant Collection Temperature Mode. *Sol. Energy* **2013**, *90*, 58–67. [[CrossRef](#)]
21. Singh, D.B.; Yadav, J.K.; Dwivedi, V.K.; Kumar, S.; Tiwari, G.N.; Al-Helal, I.M. Experimental Studies of Active Solar Still Integrated with Two Hybrid PVT Collectors. *Sol. Energy* **2016**, *130*, 207–223. [[CrossRef](#)]
22. Dupeyrat, P.; Ménézo, C.; Rommel, M.; Henning, H.-M. Efficient Single Glazed Flat Plate Photovoltaic-Thermal Hybrid Collector for Domestic Hot Water System. *Sol. Energy* **2011**, *85*, 1457–1468. [[CrossRef](#)]
23. Bhattarai, S.; Oh, J.-H.; Euh, S.-H.; Kafle, G.K.; Kim, D.H. Simulation and Model Validation of Sheet and Tube Type Photovoltaic Thermal Solar System and Conventional Solar Collecting System in Transient States. *Sol. Energy Mater. Sol. Cells* **2012**, *103*, 184–193. [[CrossRef](#)]
24. Tiwari, G.N.; Fischer, O.; Mishra, R.K.; Al-Helal, I.M. Performance Evaluation of N-Photovoltaic Thermal (PVT) Water Collectors Partially Covered by Photovoltaic Module Connected in Series: An Experimental Study. *Sol. Energy* **2016**, *134*, 302–313.
25. Santbergen, R.; Rindt, C.C.M.; Zondag, H.A.; Van Zolingen, R.J.C. Detailed Analysis of the Energy Yield of Systems with Covered Sheet-and-Tube PVT Collectors. *Sol. Energy* **2010**, *84*, 867–878. [[CrossRef](#)]
26. Li, G.; Pei, G.; Yang, M.; Ji, J. Experiment Investigation on Electrical and Thermal Performances of a Semitransparent Photovoltaic/Thermal System with Water Cooling. *Int. J. Photoenergy* **2014**, *2014*, 360235. [[CrossRef](#)]
27. Gaur, A.; Ménézo, C.; Giroux, S. Numerical Studies on Thermal and Electrical Performance of a Fully Wetted Absorber PVT Collector with PCM as a Storage Medium. *Renew. Energy* **2017**, *109*, 168–187. [[CrossRef](#)]
28. Preet, S.; Bhushan, B.; Mahajan, T. Experimental Investigation of Water Based Photovoltaic/Thermal (PV/T) System with and without Phase Change Material (PCM). *Sol. Energy* **2017**, *155*, 1104–1120. [[CrossRef](#)]

29. Othman, M.Y.; Hamid, S.A.; Tabook, M.A.S.; Sopian, K.; Roslan, M.H.; Ibarahim, Z. Performance Analysis of PV/T Combi with Water and Air Heating System: An Experimental Study. *Renew. Energy* **2016**, *86*, 716–722. [[CrossRef](#)]
30. Sharaf, O.Z.; Orhan, M.F. Concentrated Photovoltaic Thermal (CPVT) Solar Collector Systems: Part I–Fundamentals, Design Considerations and Current Technologies. *Renew. Sustain. Energy Rev.* **2015**, *50*, 1500–1565. [[CrossRef](#)]
31. Pierucci, G.; Hosouli, S.; Salvestroni, M.; Messeri, M.; Fagioli, F.; de Lucia, M. Indoor Thermal Loss Test on Small-Size Solar Receiver (UF-RT01) for Process Heat Application. *Sol. Energy Adv.* **2021**, *1*, 100010. [[CrossRef](#)]
32. Evans, D.L.; Facinelli, W.A.; Otterbein, R.T. Combined Photovoltaic/Thermal System Studies. *STIN* **1978**, *79*, 32691.
33. Xu, N.; Ji, J.; Sun, W.; Huang, W.; Jin, Z. Electrical and Thermal Performance Analysis for a Highly Concentrating Photovoltaic/Thermal System. *Int. J. Photoenergy* **2015**, *2015*, 537538. [[CrossRef](#)]
34. Quaia, S.; Lughi, V.; Giacalone, M.; Vinzi, G. Technical-Economic Evaluation of a Combined Heat and Power Solar (CHAPS) Generator Based on Concentrated Photovoltaics. In Proceedings of the International Symposium on Power Electronics Power Electronics, Electrical Drives, Automation and Motion, Sorrento, Italy, 20–22 June 2012; IEEE: New York, NY, USA, 2012; pp. 1130–1135.
35. Rosell, J.I.; Vallverdú, X.; Lechón, M.A.; Ibáñez, M. Design and Simulation of a Low Concentrating Photovoltaic/Thermal System. *Energy Convers. Manag.* **2005**, *46*, 3034–3046. [[CrossRef](#)]
36. Coventry, J.S. Performance of a Concentrating Photovoltaic/Thermal Solar Collector. *Sol. Energy* **2005**, *78*, 211–222. [[CrossRef](#)]
37. Bernardo, L.R.; Perers, B.; Håkansson, H.; Karlsson, B. Performance Evaluation of Low Concentrating Photovoltaic/Thermal Systems: A Case Study from Sweden. *Sol. Energy* **2011**, *85*, 1499–1510. [[CrossRef](#)]
38. Li, M.; Ji, X.; Li, G.L.; Yang, Z.M.; Wei, S.X.; Wang, L.L. Performance Investigation and Optimization of the Trough Concentrating Photovoltaic/Thermal System. *Sol. Energy* **2011**, *85*, 1028–1034. [[CrossRef](#)]
39. Proell, M.; Karrer, H.; Brabec, C.J.; Hauer, A. The Influence of CPC Reflectors on the Electrical Incidence Angle Modifier of C-Si Cells in a PVT Hybrid Collector. *Sol. Energy* **2016**, *126*, 220–230. [[CrossRef](#)]
40. Sharma, S.; Tahir, A.; Reddy, K.S.; Mallick, T.K. Performance Enhancement of a Building-Integrated Concentrating Photovoltaic System Using Phase Change Material. *Sol. Energy Mater. Sol. Cells* **2016**, *149*, 29–39. [[CrossRef](#)]
41. Widjolar, B.K.; Abdelhamid, M.; Jiang, L.; Winston, R.; Yablonoitch, E.; Scranton, G.; Cygan, D.; Abbasi, H.; Kozlov, A. Design, Simulation and Experimental Characterization of a Novel Parabolic Trough Hybrid Solar Photovoltaic/Thermal (PV/T) Collector. *Renew. Energy* **2017**, *101*, 1379–1389. [[CrossRef](#)]
42. Singh, D.B.; Tiwari, G.N. Performance Analysis of Basin Type Solar Stills Integrated with N Identical Photovoltaic Thermal (PVT) Compound Parabolic Concentrator (CPC) Collectors: A Comparative Study. *Sol. Energy* **2017**, *142*, 144–158. [[CrossRef](#)]
43. Singh, D.B.; Tiwari, G.N. Exergoeconomic, Enviroeconomic and Productivity Analyses of Basin Type Solar Stills by Incorporating N Identical PVT Compound Parabolic Concentrator Collectors: A Comparative Study. *Energy Convers. Manag.* **2017**, *135*, 129–147. [[CrossRef](#)]
44. EN12975-2; Thermal Solar Systems and Components-Solar Collectors. Test Methods; Slovenian Institute for Standardization: Ljubljana, Slovenia, 2006.
45. EN12976-1; Thermal Solar Systems and Components-Factory Made Systems-General Requirements. Test Methods; Slovenian Institute for Standardization: Ljubljana, Slovenia, 2006.
46. DDCEN/TS12977-1; Thermal Solar Systems and Components-Custom Built Systems-General Requirements for Solar Water Heaters and Combisystems. Test Methods; Slovenian Institute for Standardization: Ljubljana, Slovenia, 2010.
47. Norm, M. ASHRAE Standard 93. In *Methods of Testing to Determine Thermal Performance of Solar Collectors*; ASHRAE: Washington, DC, USA, 2003.
48. ASTM E905-87(2007); Standard Test Method for Determining Thermal Performance of Tracking Concentrating Solar Collectors. ASTM International: West Conshohocken, PA, USA, 2007.
49. SRCC600; Minimum Standard for Solar Thermal Concentrating Collectors. Solar Rating and Certification Corporation (SRCC): Cocoa, FL, USA, 2015.
50. ISO9806:2017; Solar Energy-Solar Thermal Collectors-Test Methods. ISO: Geneva, Switzerland, 2017.
51. Osório, T.; Carvalho, M.J. Testing of Solar Thermal Collectors under Transient Conditions. *Sol. Energy* **2014**, *104*, 71–81. [[CrossRef](#)]
52. Osório, T.; Carvalho, M.J. Testing of Solar Thermal Collectors under Transient Conditions. *Energy Procedia* **2012**, *30*, 1344–1353. [[CrossRef](#)]
53. Fernández-García, A.; Valenzuela, L.; Zarza, E.; Rojas, E.; Pérez, M.; Hernández-Escobedo, Q.; Manzano-Agugliaro, F. SMALL-SIZED Parabolic-Trough Solar Collectors: Development of a Test Loop and Evaluation of Testing Conditions. *Energy* **2018**, *152*, 401–415. [[CrossRef](#)]
54. IEEE1262; IEEE Recommended Practice for Qualification of Photovoltaic (PV) Modules. IEEE: New York, NY, USA, 1995.
55. IEEE929; IEEE Recommended Practice for Utility Interface of Photovoltaic (PV) Systems. IEEE: New York, NY, USA, 2000.
56. UL1703; UL Standard for Safety Flat-Plate Photovoltaic Modules and Panels. UL: Northbrook, IL, USA, 1993.
57. UL1741; UL Standard for Safety Inverters, Converters, Controllers and Interconnection System Equipment for Use with Distributed Energy Resources. UL: Northbrook, IL, USA, 2010.
58. UL4703; Photovoltaic Wire. UL: Northbrook, IL, USA, 2005.
59. IEC61215; Crystalline Silicon Terrestrial Photovoltaic (PV) Modules–Design Qualification and Type Approval. IEC: Geneva, Switzerland, 2005.

60. IEC61646; Thin-Film Terrestrial Photovoltaic (PV) Modules—Design Qualification and Type Approval. IEC: Geneva, Switzerland, 2008.
61. IEC61730-1; Photovoltaic (PV) Module Safety Qualification Part 1: Requirements for Construction. IEC: Geneva, Switzerland, 2004.
62. IEC61730-2; Photovoltaic (PV) Module Safety Qualification Part 2: Requirements for Testing. IEC: Geneva, Switzerland, 2004.
63. Adsten, M.; Helgesson, A.; Karlsson, B. Evaluation of CPC-Collector Designs for Stand-Alone, Roof- or Wall Installation. *Sol. Energy* **2005**, *79*, 638–647. [[CrossRef](#)]
64. Solarus Website. Available online: www.solarus.com (accessed on 4 December 2018).
65. Rönnelid, M.; Perers, B.; Karlsson, B. Construction and Testing of a Large-Area CPC-Collector and Comparison with a Flat Plate Collector. *Sol. Energy* **1996**, *57*, 177–184. [[CrossRef](#)]
66. Osório, T. Solar Thermal Collectors under Transient Conditions: Optical and Thermal Characterization Based on the Quasi-Dynamic Model. 2011. Available online: <https://www.semanticscholar.org/paper/Solar-thermal-collectors-under-transient-conditions-Os%C3%B3rio/987aad43a437568371697ac5e6c15f5703b4d70d> (accessed on 8 January 2023).
67. Fischer, S.; Lüpfert, E.; Müller-Steinhagen, H. Efficiency Testing of Parabolic Trough Collectors Using the Quasi-Dynamic Test Procedure According to the European Standard EN 12975. In Proceedings of the SolarPACES 13th Symposium on Concentrating Solar Power and Chemical Energy Technologies, Seville, Spain, 20–23 June 2006.
68. Janotte, N.; Lüpfert, E.; Pitz-Paal, R.; Pottler, K.; Eck, M.; Zarza, E.; Riffelmann, K.-J. Influence of Measurement Equipment on the Uncertainty of Performance Data from Test Loops for Concentrating Solar Collectors. *J. Sol. Energy Eng.* **2010**, *132*, 031003. [[CrossRef](#)]
69. Dieck, R.H. *Measurement Uncertainty: Methods and Applications*; ISA: Atlanta, GA, USA, 2007; ISBN 1556179154.
70. Sabatelli, V.; Marano, D.; Braccio, G.; Sharma, V.K. Efficiency Test of Solar Collectors: Uncertainty in the Estimation of Regression Parameters and Sensitivity Analysis. *Energy Convers. Manag.* **2002**, *43*, 2287–2295. [[CrossRef](#)]
71. Kurdia, A.; Gomes, J.; Pius, G.; Ollas, P.; Olsson, O. Quasi-Dynamic Testing of a Novel Concentrating Photovoltaic Solar Collector According to ISO 9806: 2013. In Proceedings of the 12th International Conference on Solar Energy for Buildings and Industry (ISES EuroSun), Rapperswil, Switzerland, 10–13 September 2018; International Solar Energy Society: Freiburg im Breisgau, Germany, 2018; pp. 1262–1273.
72. Hosouli, S.; Gomes, J.; Loris, A.; Pazmiño, I.A.; Naidoo, A.; Lennermo, G.; Mohammadi, H. Evaluation of a solar photovoltaic thermal (PVT) system in a dairy farm in Germany. *Sol. Energy Adv.* **2023**, *3*, 100035. [[CrossRef](#)]

Disclaimer/Publisher’s Note: The statements, opinions and data contained in all publications are solely those of the individual author(s) and contributor(s) and not of MDPI and/or the editor(s). MDPI and/or the editor(s) disclaim responsibility for any injury to people or property resulting from any ideas, methods, instructions or products referred to in the content.